

Examination of the Partial Discharge Behaviour Within a Spherical Cavity in Insulation Paper of Transformer

Muhammad Hakirin Roslan^{1,2}, Norhafiz Azis^{2,3*}, Mohd Zainal Abidin Ab Kadir²,
Jasronita Jasni² and Mohd Fairouz Mohd Yousof⁴

¹Faculty of Engineering, Universiti Pertahanan Nasional Malaysia, 57000 Kem Sg Besi, Malaysia

²Advanced Lightning, Power and Energy Research Centre (ALPER), Universiti Putra Malaysia, 43400 UPM, Serdang, Selangor, Malaysia

³Institute of Nanoscience and Nanotechnology (ION2), Universiti Putra Malaysia, 43400 UPM, Serdang, Selangor, Malaysia

⁴Faculty of Electrical and Electronics Engineering, Universiti Tun Hussein Onn Malaysia, 86400 UTHM, Parit Raja, Johor, Malaysia

ABSTRACT

This paper investigates the behaviour of partial discharge (PD) in transformer insulation paper based on the Finite Element Method (FEM). The three-dimensional (3D) FEM model consists of conductor and insulation paper, representing part of a transformer's high voltage winding. The conductor's width, height, and length used in this study were 2.4 mm, 11.5 mm, and 16 mm. An insulation paper thickness of 1 mm was modelled around the conductor. An internal cavity with a diameter of 0.5 mm cavity was introduced within the insulation paper. This study introduced two locations of the spherical cavities at the centre and left corner of the insulation paper: Location 1 (L1) and Location 2 (L2). An AC voltage of 33 kV, 50 Hz, was applied to the conductor while the bottom of the insulation paper was grounded. The model was used to study the electric field distribution within the insulation

paper and its effect on PD current and charge magnitude. The influence of cavity location on the charge magnitude was also examined. It is found that the electric field distribution is influenced by the conductor configuration as well as the location of the cavity. The electric field in the cavity is the highest at L1 compared to L2. The first PD occurs faster for the cavity with a high electric field. Due to the PD occurrence at the same inception field, the real PD current

ARTICLE INFO

Article history:

Received: 16 June 2022

Accepted: 13 September 2022

Published: 31 March 2023

DOI: <https://doi.org/10.47836/pjst.31.3.05>

E-mail addresses:

hakirin@upnm.edu.my (Muhammad Hakirin Roslan)

norhafiz@upm.edu.my (Norhafiz Azis)

mzk@upm.edu.my (Mohd Zainal Abidin Ab Kadir)

jas@upm.edu.my (Jasronita Jasni)

fairouz@uthm.edu.my (Mohd Fairouz Mohd Yousof)

* Corresponding author

and charge magnitude is similar at different locations. The apparent PD current and charge magnitude induced at the ground electrode is slightly higher at L1 than at L2.

Keywords: Insulation paper, partial discharge modelling, spherical cavity, transformer

INTRODUCTION

Among the critical equipment in the electrical power system network is transformers. Transformers can be subjected to different types of electrical issues, which can reduce their reliabilities. One common issue in the insulation of transformers is Partial Discharge (PD) (Hussain et al., 2021). PD is an electrical discharge that originates from a defective area within the insulation system (Naidu & Kamaraju, 2013). During the PD occurrence, solid insulation can degrade over time and extend to full electrical discharge. The most known defective areas are the void, cavity, and crack in the solid insulation (E-CIGRE, 2017). In recent years, PD assessment has become an important tool for evaluating the integrity of transformer insulation. Generally, the PD phenomenon is quite complex and requires further analyses through modelling the physical process. The electric field distributions before and after PD can be further evaluated based on the analyses.

The PD models with regard to a spherical cavity within solid dielectric material can be categorized into three capacitance, induced charge concept (ICC) and Finite Element Method (FEM) models (Illias et al., 2017). The three-capacitance or ABC model represents the model of PD as a capacitance circuit (Whitehead, 1952). This model is simple; however, the surface charge decay and charge accumulation along the cavity surface are not considered in the analysis. The PD occurrence of this model does not relate to the changes in capacitance as in the ICC model. The ICC model is derived based on the phenomenon of charge distribution on the cavity surface due to PD (Pedersen et al., 1995; Pedersen et al., 1991). The ICC model is also known as the analytical equation PD model, which is based on streamer-type PD whereby consideration on the surface charge accumulation on the cavity surface due to a PD occurrence is considered. The simulation time for the ICC model is short, but it is only suitable if the cavity size is small and has a uniform field distribution.

In recent years, the FEM model has been widely used for the PD model of a spherical cavity (Borghei et al., 2021; Illias et al., 2009, 2010, 2011a, 2011b, 2011c; Illias et al., 2012a; Illias et al., 2012b; Illias et al., 2015a, 2015b). This approach is promising for developing the PD model since it can be simulated dynamically. The FEM model solves the electric field distribution in a cavity numerically and can be applied to solve non-uniform electric field distribution. The electric field distribution during the PD process can also be obtained through the FEM model. The apparent and real charges based on the FEM model are also comparable with the experimental data (Borghei et al., 2021; Forssén & Edin, 2008; Illias, 2011; Illias et al., 2012a). The FEM model can be considered a reliable tool to simulate PD due to its credibility in simulating PD in complex geometry. The FEM

model has also been applied to examine the PD activities in cables (Anagha et al., 2018; Joseph et al., 2019).

This paper presents the investigation of PD behaviour within a spherical cavity in the insulation paper of a transformer through FEM modelling. The 3D model consists of a conductor, insulation paper and a spherical cavity, whereby it is developed and solved through a transient electric solver. The electric field distribution in the insulation paper with consideration of the spherical cavity is evaluated, and its effect on the PD current and charge magnitude is examined.

PARTIAL DISCHARGE MODELLING

Two important criteria need to be considered for PD modelling:

1. The electric field in the cavity should exceed the cavity PD inception field, E_{inc} .
2. The presence of the free electron initiates the ionization process.

The discharge process of PD can be delayed if there is no presence of the free electron, even though the electric field already exceeds the E_{inc} . Thus, the free electron in the cavity is a crucial parameter to initiate PD. The Electron Generation Rate (EGR) controls the number of free electrons in the cavity. Two main contributions of EGR are surface emission and volume ionization. Once all the requirements were satisfied, the discharge process simulation was initiated to model the PD occurrence. The simulation continued until the cavity's electric field was lower than the PD extinction field, E_{ext} .

PD Physical Parameter

Four parameters need to be acquired to model the PD. These parameters are known as the physical process parameter, which consists of the E_{inc} , E_{ext} , EGR and surface charge decay.

PD Inception Field. E_{inc} was determined based on Equation 1, where the PD was considered a streamer type (Borghei et al., 2021; Niemeyer, 1995; Pan et al., 2019).

$$E_{inc} = \left(\frac{E_1}{P}\right)_{cr} P \left(1 + \frac{B}{\sqrt{Pd}}\right) \quad [1]$$

In the case of air, the ionization parameters for $(E_1/p)_{cr}$ and B are defined as $24.2 \text{ VPa}^{-1} \text{ m}^{-1}$ and 8.6, respectively (Illias, 2011). P and d are the pressure and diameter of the cavity, respectively. Equation 1 can be simplified into Equation 2 if the cavity contains air.

$$E_{inc} = 24.2P \left(1 + \frac{8.6}{\sqrt{Pd}}\right) \quad \text{unit in } \frac{\text{V}}{\text{m}} \quad [2]$$

The pressure and diameter of the cavity were set to 100 kPa and 0.5 mm. Based on Equation 2, the computed E_{inc} was 5.4 kV/mm.

PD Extinction Field. E_{ext} is the minimum electric field required to stop the discharge process during the PD occurrence. E_{ext} was determined based on Equation 3, where the value was set to 10% of E_{inc} obtained from Equation 2 (Joseph et al., 2019).

$$E_{ext} = 0.1E_{inc} \quad \text{unit in } \frac{V}{m} \quad [3]$$

Electron Generation Rate (EGR). EGR in the cavity is one of the crucial parameters that control the condition of PD occurrence. The free electron must exist in the cavity to start the ionization process. The lack of the free electron will delay the PD occurrence even if the first condition of the cavity E_{inc} is already satisfied. The delay time from the time occurrence of E_{inc} to the time of PD occurrence was defined as statistical time lag, τ_{stat} . The EGR affects the τ_{stat} , which is contributed by the cavity surface emission and volume ionization (Illias et al., 2015a). The EGR contributed by the volume ionization was considered since only the first discharge was simulated in this study, whereby the free electron was always considered available. There was no free electron contributed by the surface emission and the surface charge decay effect since the subsequent discharge was not simulated in this study.

Discharge Process

Two methods to develop the discharge process during PD occurrence based on the FEM model are electrostatic and electric transient (Illias et al., 2017). This study used the electric transient method to model the discharge process based on the conductance model. The discharge channel was included in the model due to the high charge development in the cavity. As a result, the discharge process influenced the entire cavity, which increased the cavity conductivity from the initial value to a high value during the PD occurrence. It will lead to the decrement of the electric field in the cavity. Once the electric field in the cavity was less than the E_{ext} , the conductivity of the whole cavity was set to non-conducting. Figure 1 shows the flowchart of the discharge model for the first PD.

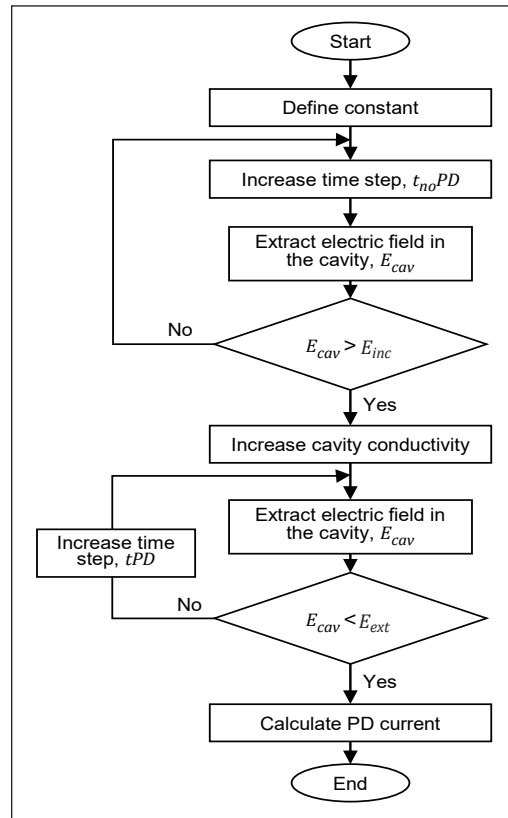


Figure 1. Flowchart of the discharge model

Model Geometry

Figure 2 shows the three-dimensional (3D) FEM model geometry of the insulation paper and conductor in Ansys Maxwell. The transient electric solver was used to solve the electric potential distribution in insulation paper. The model was modelled based on the part of the disc layered high voltage winding in a 33/11 kV, 30 MVA transformer.

The model consisted of conductor and insulation paper. To represent the defect area, a diameter of 0.5 mm cavity was located within the insulation paper. The detail of the geometrical design can be seen in Table 1 (Murthy et al., 2020).

In this study, there were two locations of the cavities, namely Location 1 (L1) and Location 2 (L2), as shown in Figure 3. L1 is the location of the cavity at the centre of the insulation paper, and L2 is the location of the cavity at the left corner of the insulation paper.

Simulation of Model

The electric potential calculation in the model was performed through the transient electric solver. The details of the other parameters for the simulation are shown in Table 2. A 33 kV, 50 Hz AC was supplied at the conductor while the bottom of the insulation paper was grounded. The simulation time was set to 100 μ s during no PD to reduce the simulation time while maintaining the accuracy of the electric field in one time step. The time step during the occurrence of PD was set to 1 ns to maximize the accuracy in one time step due to the sudden reduction of the electric field in the cavity once the PD was initiated. The fast change in the electric field within the cavity was controlled by the conductivity during the

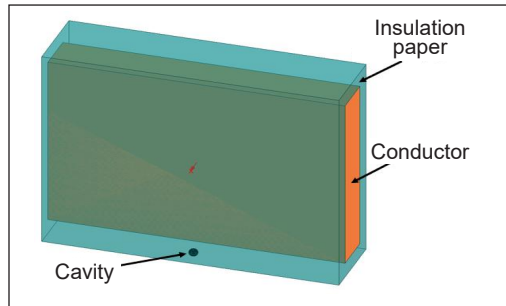


Figure 2. 3D FEM model of insulation paper and conductor of high voltage winding

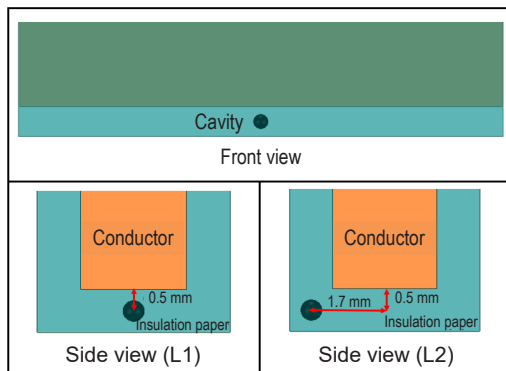


Figure 3. Two different cavity locations within the insulation paper

Table 1
Parameters for 3D Finite Element Method model

Parameters	Values
Power rating	30 MVA
High voltage winding rating	33 kV
Low voltage winding rating	11 kV
Height (conductor)	11.5 mm
Width (conductor)	2.4 mm
Length (conductor)	16 mm
The thickness of the insulation paper	1 mm
Cavity diameter	0.5 mm

discharge process. In this study, the conductivity during PD was set to 0.005 s/m to reduce the simulation time and avoid the fast reduction of the electric field. The apparent and real charges were determined based on the current integration flowing through the electrode and cavity centre surface area, as shown in Equations 4 - 7 (Borghei et al., 2021).

$$I_{real}(t) = \int_{S_{cav}} \overrightarrow{J(t)} \cdot \vec{n} \, dS \quad [4]$$

$$I_{app}(t) = \int_{S_{ground}} \overrightarrow{J(t)} \cdot \vec{n} \, dS \quad [5]$$

$$Q_{real} = \int_{t_{inc}}^{t_{ext}} I_{real}(t) \, dt \quad [6]$$

$$Q_{app} = \int_{t_{inc}}^{t_{ext}} I_{app}(t) \, dt \quad [7]$$

Where $\overrightarrow{J(t)}$ is the current density, S_{cav} is the cavity centre surface area, and S_{ground} is the ground electrode surface area. The t_{inc} and t_{ext} are the time occurrence of the inception and extinction fields.

Table 2
Parameter for partial discharge modelling of the insulation paper and cavity

Parameters	Values	Units
Insulation paper (relative permittivity), ϵ_{mat}	2.3	
Cavity (relative permittivity), ϵ_{cav}	1	
Insulation paper (conductivity), σ_{mat}	1×10^{-10}	s/m
Conductivity of cavity during no PD, $\sigma_{cav,0}$	0	s/m
Conductivity of cavity during PD, $\sigma_{cav,PD}$	5×10^{-3}	s/m
Simulation time step (no PD), t_{noPD}	100	μ s
Simulation time step during PD, t_{PD}	1	ns

RESULTS AND DISCUSSION

Electric Field Distribution in the Paper Insulation for Different Locations of the Cavity

The electric field distribution in the insulation paper before the occurrence of the PD for the cavity at L1 can be seen in Figure 4. The electric field distribution at the centre of the cavity is higher than the insulation paper. It is expected since the cavity's relative permittivity is lower than the insulation paper. Since the cavity surface at the top and bottom is near the

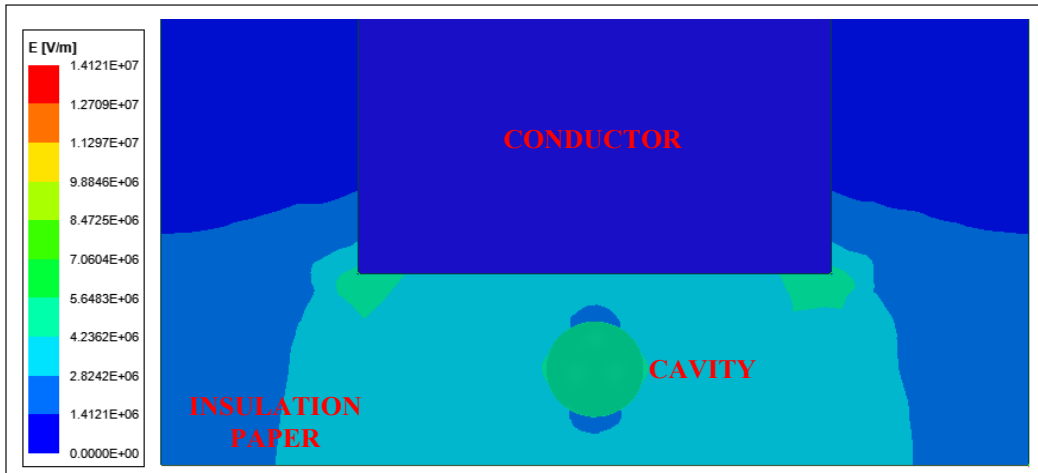


Figure 4. Electric field distribution before PD occurrence for cavity location at L1

electrode, the electric field distribution in the insulating paper is low at the top and bottom of the cavity surface. The electric field around the edges of the conductor is higher than the left and right of the insulation paper.

After the occurrence of the PD, the electric field inside the cavity rapidly decreases, as shown in Figure 5. It is due to the cavity conductivity being higher than the initial value during the discharge process. The highest electric fields are located at the top and bottom surfaces of the cavity. The conductor edge affects the electric field distribution in the insulation paper, which is higher at the centre than at the left and right of the insulation paper.

The electric field distribution in the insulation paper before the PD occurrence for the cavity at L2 is shown in Figure 6. The electric field distribution is higher at the centre of the insulation paper. It is due to the influence of the sharp edge of the conductor. The electric field in the cavity is slightly lower than the centre of the insulation paper since the cavity is slightly far from the centre of the insulation paper.

A similar pattern of the electric field distribution in the cavity compared to Figure 5 is found after the PD occurrence, as shown in Figure 7. During the PD occurrence, the cavity conductivity increases, allowing the PD pulse current to appear, which results in the electric field reduction in the cavity. The electric field distribution at the top surface of the cavity has a similar pattern in Figure 5, whereby the highest electric field is at the right of the conductor's edge.

The sharp edge of the conductor and the location of the cavity within the insulation paper can affect the electric field distribution in the system. Figure 8 shows the electric field in the cavity without the PD activity for one cycle. At the same electric potential injected at the conductor, the electric field at L1 is slightly higher than at L2. The time to reach the

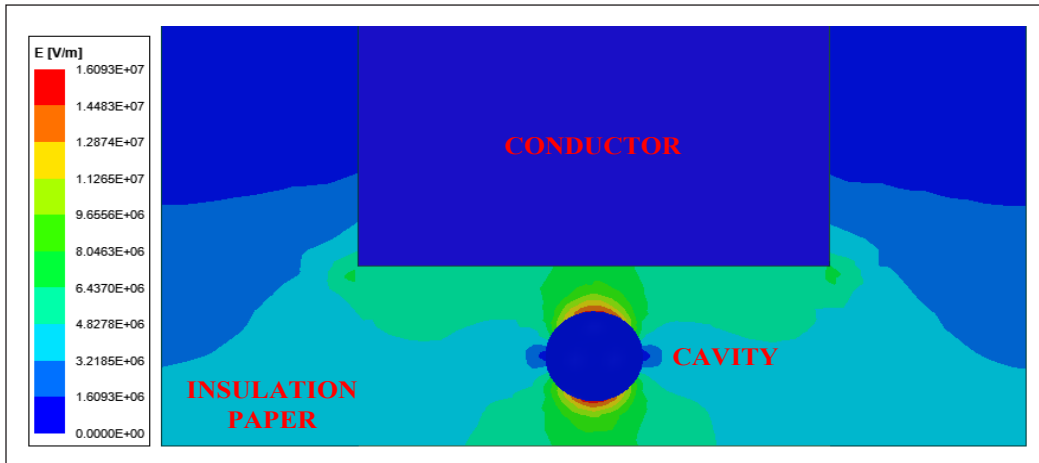


Figure 5. Electric field distribution after PD occurrence for cavity location at L1

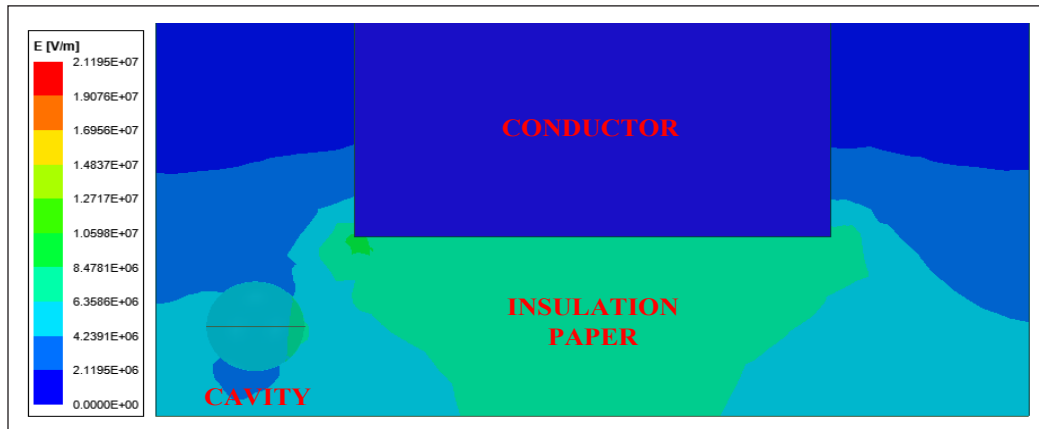


Figure 6. Electric field distribution before PD occurrence for cavity location at L2

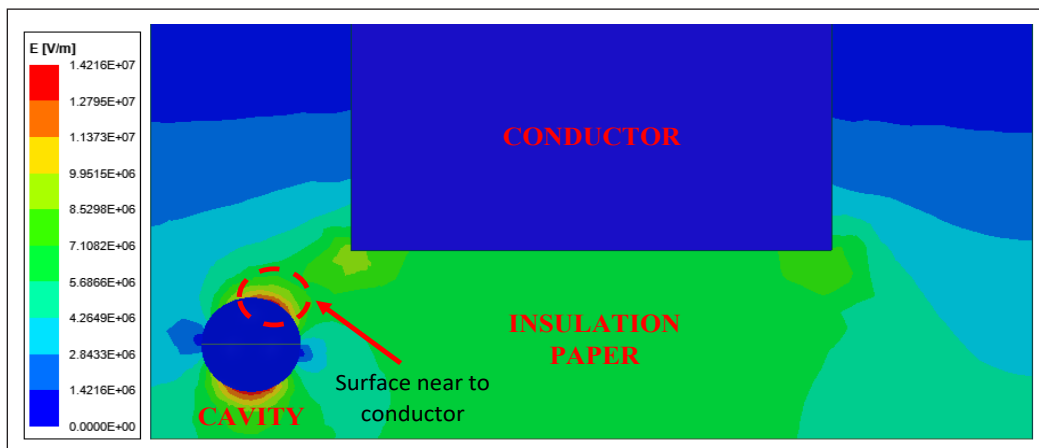


Figure 7. Electric field distribution after PD occurrence for cavity location at L2

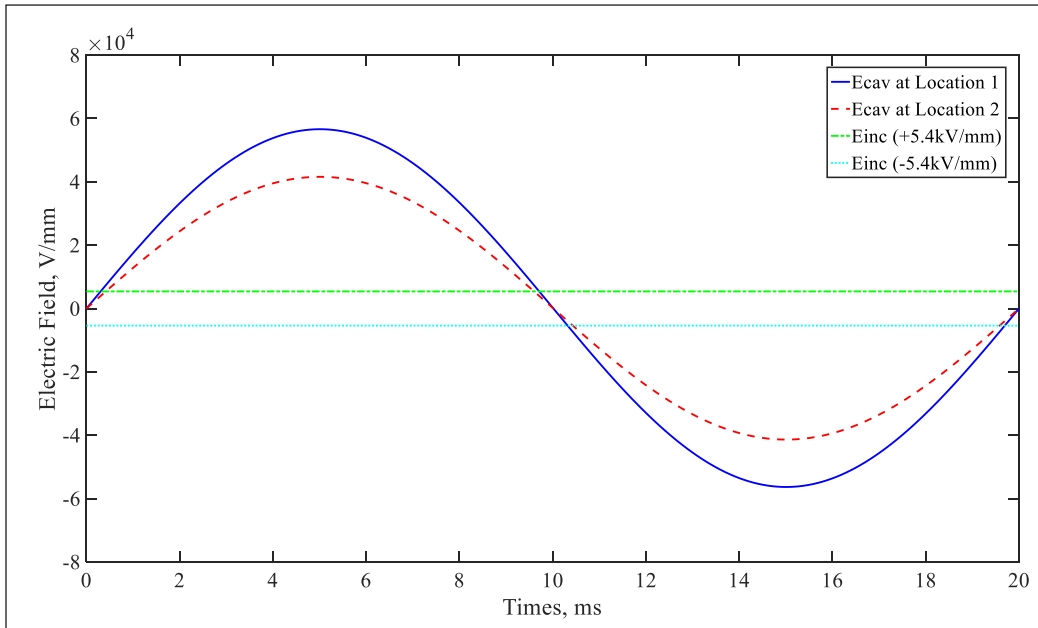


Figure 8. Electric field in the cavity versus time for one cycle in the absence of PD activity

E_{inc} is faster at L1 than at L2. It is due to the sharp edge of the conductor as well as the location of the cavity in the insulation paper.

PD Current and First Discharge Magnitude as A Function of Cavity Location

The simulated real and apparent PD currents for different cavity locations can be seen in Figure 9. The real PD current recorded at L1 is close to L2 since the first PD occur at the same E_{inc} due to the same cavity size. However, the PD occurrence time is different because the electric field in the cavity at L1 is slightly higher than at L2, which can be seen in Figure 8. The simulated apparent PD current at L1 is slightly higher than at L2. The difference is affected by the cavity’s location and the electric field distribution in the insulation paper.

The simulated real and apparent charge magnitudes for different cavity locations are shown in Figure 10. The charge magnitude was obtained from the integrated PD current. The real and apparent charges range for both locations from 0.015 to 0.05 nC. The electric field distribution in the insulation paper affects the apparent charge magnitude induced at the ground electrode, where its value at L2 is slightly lower than L1. The real charge magnitude is close at both locations.

The electric field distribution in the insulation paper is influenced by the shape of the conductor as well as the electric field in the cavity, which depends on the cavity’s location. The highest electric field distribution is found at the centre of the insulation

paper, which is close to the sharp edges of the conductor. The electric field in the cavity at L1 is the highest. The shape of the conductor is expected to affect the subsequent PD and its intensity due to its influence on the electric field distribution in insulation paper. The location of the cavity can also affect the PD current and charge magnitude due to the differences in the electric field distribution.

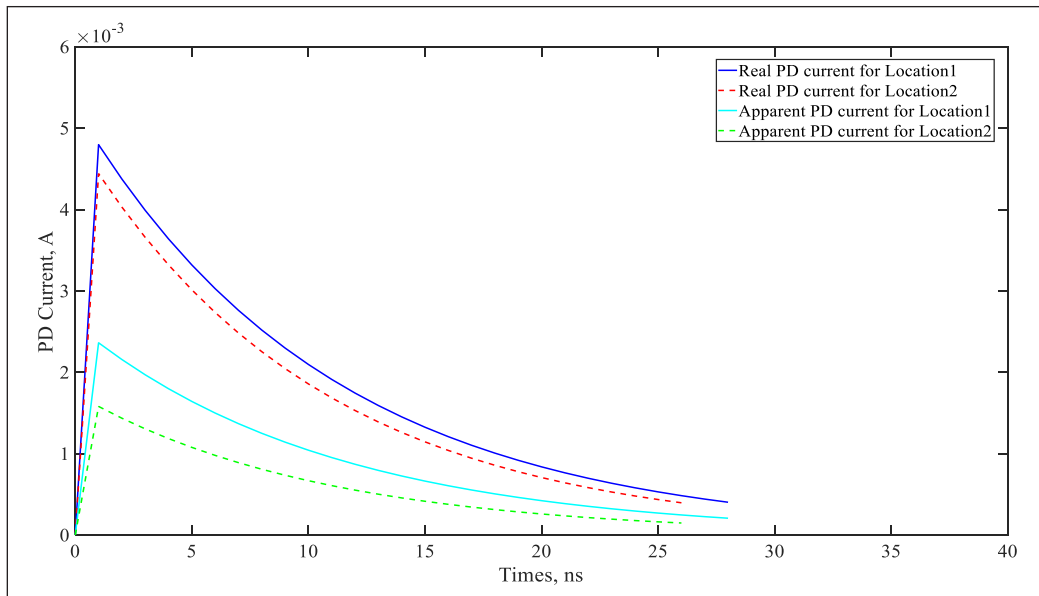


Figure 9. Real and apparent PD current for different cavity locations

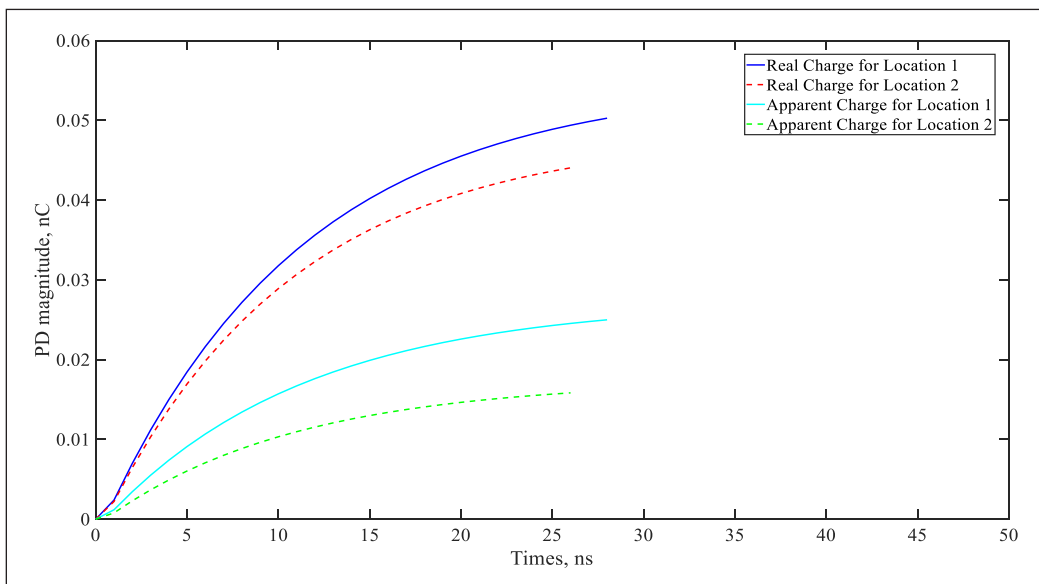


Figure 10. Real and apparent charge magnitudes for different cavity locations

CONCLUSION

In conclusion, PD modelling based on FEM can be used to examine the behaviour of PD in terms of electric field distribution as well as PD current and charge magnitude within a spherical cavity in the insulation paper of the transformer. The electric field distribution in the insulation paper is affected by the sharp edge of the electrode. This condition causes the electric field in the cavity to change dependent on the location of the cavity. The cavity location affects the first apparent PD current and charge magnitude induced at the ground electrode. The real PD current and charge magnitude of the first PD is similar at both cavity locations due to the PD occurrence at the same E_{inc} . The cavity location can affect the time of PD occurrence, whereby L1 is faster than L2.

ACKNOWLEDGMENT

The authors would like to express their sincere gratitude for the funding by the Matching Grant Universiti Putra Malaysia-Kyushu Institute of Technology (UPM.RMC/800/2/2/4/ Matching UPM-KYUTECH/2021/ 9300481). Special thanks to Advanced Lightning, Power and Energy Research (ALPER), UPM, for technical support to this research.

REFERENCES

- Anagha, E. R., Joseph, J., & Sindhu, T. K. (2018). *A finite element method based approach for modeling of partial discharges in HVDC cables*. In *2018 Electrical Insulation Conference (EIC)* (pp. 533-537). IEEE Publishing. <https://doi.org/10.1109/EIC.2018.8481089>
- Borghesi, M., Ghassemi, M., Rodriguez-Serna, J. M., & Albarracin-Sanchez, R. (2021). A finite element analysis and an improved induced charge concept for partial discharge modeling. *IEEE Transactions on Power Delivery*, *36*(4), 2570-2581. <https://doi.org/10.1109/tpwrd.2020.2991589>
- E-CIGRE. (2017). *Partial Discharges in Transformers*. e-cigre.org. <https://e-cigre.org/publication/676-partial-discharges-in-transformers>
- Forssén, C., & Edin, H. (2008). Partial discharges in a cavity at variable applied frequency part 2: Measurements and modeling. *IEEE Transactions on Dielectrics and Electrical Insulation*, *15*(6), 1610-1616. <https://doi.org/10.1109/TDEI.2008.4712664>
- Hussain, M. R., Refaat, S. S., & Abu-Rub, H. (2021). Overview and partial discharge analysis of power transformers: A literature review. *IEEE Access*, *9*, 64587-64605. <https://doi.org/10.1109/access.2021.3075288>
- Illias, H. A., Chen, G., & Lewin, P. L. (2017). Comparison between three-capacitance, analytical-based and finite element analysis partial discharge models in condition monitoring. *IEEE Transactions on Dielectrics and Electrical Insulation*, *24*(1), 99-109. <https://doi.org/10.1109/tdei.2016.005971>
- Illias, H. A., Tunio, M. A., Mokhlis, H., Chen, G., & Bakar, A. H. A. (2015a). Determination of partial discharge time lag in void using physical model approach. *IEEE Transactions on Dielectrics and Electrical Insulation*, *22*(1), 463-471. <https://doi.org/10.1109/tdei.2014.004618>

- Illias, H. A., Tunio, M. A., Mokhlis, H., Chen, G., & Bakar, A. H. A. (2015b). Experiment and modeling of void discharges within dielectric insulation material under impulse voltage. *IEEE Transactions on Dielectrics and Electrical Insulation*, 22(4), 2252-2260. <https://doi.org/10.1109/tdei.2015.004817>
- Illias, H. A., Chen, G., & Lewin, P. L. (2012a). Partial discharge within a spherical cavity in a dielectric material as a function of cavity size and material temperature. *IET Science, Measurement & Technology*, 6(2), 52-62. <https://doi.org/10.1049/iet-smt.2011.0091>
- Illias, H. A., Jian, L. T., Bakar, A. H. A., & Mokhlis, H. (2012b). Partial discharge simulation under various applied voltage waveforms. In *2012 IEEE International Conference on Power and Energy (PECon)*, (pp. 967-972). IEEE Publishing. <https://doi.org/10.1109/PECon.2012.6450358>
- Illias, H. A. (2011). *Measurement and simulation of partial discharges within a spherical cavity in a solid dielectric material* [Doctoral dissertation]. University of Southampton, UK. <https://eprints.soton.ac.uk/194921/>
- Illias, H. A., Chen, G., & Lewin, P. L. (2011a). The influence of spherical cavity surface charge distribution on the sequence of partial discharge events. *Journal of Physics D: Applied Physics*, 44(24), 245202. <https://doi.org/10.1088/0022-3727/44/24/245202>
- Illias, H. A., Chen, G., & Lewin, P. L. (2011b). Partial discharge behavior within a spherical cavity in a solid dielectric material as a function of frequency and amplitude of the applied voltage. *IEEE Transactions on Dielectrics and Electrical Insulation*, 18(2), 432-443. <https://doi.org/10.1109/TDEI.2011.5739447>
- Illias, H. A., Chen, G., & Lewin, P. L. (2011c). Partial discharge behaviour within two spherical cavities in a dielectric material. In *2011 Annual Report Conference on Electrical Insulation and Dielectric Phenomena* (pp. 456-459). IEEE Publishing. <https://doi.org/10.1109/CEIDP.2011.6232693>
- Illias, H. A., Chen, G., & Lewin, P. L. (2010). Comparison of partial discharge measurement and simulation results for spherical cavities within solid dielectric materials as a function of frequency using finite element analysis method. In *2010 IEEE International Symposium on Electrical Insulation* (pp. 1-5). IEEE Publishing. <https://doi.org/10.1109/ELINSL.2010.5549733>
- Illias, H. A., Chen, G., & Lewin, P. L. (2009). Partial discharge measurements for spherical cavities within solid dielectric materials under different stress and cavity conditions In *2009 Annual Report Conference on Electrical Insulation and Dielectric Phenomena* (pp. 388-391). IEEE Publishing. <https://doi.org/10.1109/CEIDP.2009.5377831>
- Joseph, J., Mohan, S., & Krishnan, S. T. (2019). Numerical modelling, simulation and experimental validation of partial discharge in cross-linked polyethylene cables. *IET Science, Measurement & Technology*, 13(2), 309-317. <https://doi.org/10.1049/iet-smt.2018.5248>
- Murthy, A. S., Azis, N., Jasni, J., Othman, M. L., Yousof, M. F. M., & Talib, M. A. (2020). Extraction of winding parameters for 33/11 kV, 30 MVA transformer based on finite element method for frequency response modelling. *PLoS One*, 15(8), Article e0236409. <https://doi.org/10.1371/journal.pone.0236409>
- Naidu, M. S., & Kamaraju, V. (2013). *High Voltage Engineering*. McGraw Hill.
- Niemeyer, L. (1995). A generalized approach to partial discharge modeling. *IEEE Transactions on Dielectrics and Electrical Insulation*, 2(4), 510-528. <https://doi.org/10.1109/94.407017>

- Pan, C., Chen, G., Tang, J., & Wu, K. (2019). Numerical modeling of partial discharges in a solid dielectric-bounded cavity: A review. *IEEE Transactions on Dielectrics and Electrical Insulation*, 26(3), 981-1000. <https://doi.org/10.1109/tdei.2019.007945>
- Pedersen, A., Crichton, G. C., & McAllister, I. W. (1995). The functional relation between partial discharges and induced charge. *IEEE Transactions on Dielectrics and Electrical Insulation*, 2(4), 535-543. <https://doi.org/10.1109/94.407019>
- Pedersen, A., Crichton, G. C., & McAllister, I. W. (1991). The theory and measurement of partial discharge transients. *IEEE Transactions on Electrical Insulation*, 26(3), 487-497. <https://doi.org/10.1109/14.85121>
- Whitehead, S. (1952). Electrical breakdown of solids. *Nature*, 170, Article 219. <https://doi.org/10.1038/170219a0>

